Biosensors and Bioelectronics 256 (2024) 116275

Contents lists available at ScienceDirect

Biosensors and Bioelectronics

journal homepage: www.elsevier.com/locate/bios

Perovskite hydroxide-based laccase mimics with controllable activity for environmental remediation and biosensing

Yufeng Liu [a], Jing Zhang [a], Shuai Cui [a], Hui Wei [b,c,*], Dongzhi Yang [a,**]

[a] Jiangsu Key Laboratory of New Drug Research and Clinical Pharmacy, Xuzhou Medical University, Xuzhou, Jiangsu, 221002, China
[b] Department of Biomedical Engineering, College of Engineering and Applied Sciences, Nanjing National Laboratory of Microstructures, Jiangsu Key Laboratory of Artificial Functional Materials, Nanjing University, Nanjing, Jiangsu, 210023, China
[c] State Key Laboratory of Analytical Chemistry for Life Science, School of Chemistry and Chemical Engineering, Chemistry and Biomedicine Innovation Center (ChemBIC), Nanjing University, Nanjing, Jiangsu, 210023, China

ARTICLE INFO

Keywords:
Laccase mimics
Controllable activity
Environmental remediation
Neurotransmitters biosensing

ABSTRACT

Constructing relatively inexpensive nanomaterials to simulate the catalytic performance of laccase is of great significance in recent years. Although research on improving laccase-like activity by regulating ligands of copper (amino acids or small organic molecules, etc.) have achieved remarkable success. There are few reports on improving laccase-like activity by adjusting the composition of metal Cu. Here, we used perovskite hydroxide AB $(OH)_6$ as a model to evaluate the relationship between Cu based alloys and their laccase-like activity. We found that when the Cu/Mn alloy ratio of the perovskite hydroxide A point is greater than 1, the laccase-like activity of the binary alloy perovskite hydroxide is higher than that of the corresponding single Cu. Based on the measurements of XPS and ICP-MS, we deduced that the improvements of laccase-like activity mainly attribute to the ratio of $Cu^{+}/Cu^{2+}$and the content of Cu. Moreover, two types of substrates (toxic pollutants and catechol neurotransmitters) were used to successfully demonstrated such nanozymes' excellent environmental protecting function and biosensing property. This work will provide a novel approach for the construction and application of laccase-like nanozymes in the future.

1. Introduction

Laccase is one of the few natural enzymes that can be used in organic solvent environments (Mogharabi and Faramarzi, 2014; Witayakran and Ragauskas, 2009). They are often used to oxidize various phenolic substrates and have attracted much attentions from environmental protection and food industry (Minussi et al., 2002; Strong and Claus, 2011; Mayer and Staples, 2002; Couto and Herrera, 2006). However, laccase mainly exists in plants, fungi and bacteria, and the production cost of its extraction and purification is still high. While laccase can remain active in organic solvents, its protein-based component still loses activity in more stringent industrial reaction systems, such as high temperatures or high ionic strength. To this end, it is necessary to develop laccase alternatives that are low-cost, have excellent activity, high stability, and have the potential for large-scale production.

Designing and constructing artificial enzymes that mimic the structure and function of enzymes in nature is of great interest (Wulff and Liu, 2012; Dong et al., 2012; Nath et al., 2016). With the explosive development in the field of nanoscience, numerous nanomaterials have been reported to have catalytic activities similar to those of natural enzymes (called nanozymes) (Gao et al., 2007; Huang et al., 2019a, 2019b; Chen et al., 2012; Natalio et al., 2012; Liu et al., 2019; Wang et al., 2021, 2024a; Yu et al., 2024; Hou et al., 2024; Han et al., 2022; Zhang et al., 2023). Compared with natural enzymes, nanozymes have the advantages of more stable activity, lower cost, and richer functions (Zhang et al., 2021). They have shown excellent applications in the fields such as biomedical engineering, analytical sensing, environmental protection, and agriculture (Jiang et al., 2019; Li et al., 2019, 2021; Meng et al., 2020; Cui et al., 2022; Wang et al., 2024b; Ma et al., 2024; Fang et al., 2023). Therefore, constructing nanozymes with laccase-like activity is a promising approach to establish laccase alternatives.

To date, nanomaterials with laccase-like catalytic activity mainly

* Corresponding author. Department of Biomedical Engineering, College of Engineering and Applied Sciences, Nanjing National Laboratory of Microstructures, Jiangsu Key Laboratory of Artificial Functional Materials, Nanjing University, Nanjing, Jiangsu, 210023, China.
** Corresponding author.
E-mail addresses: weihui@nju.edu.cn (H. Wei), dongzhiy@xzhmu.edu.cn (D. Yang).

https://doi.org/10.1016/j.bios.2024.116275
Received 14 February 2024; Received in revised form 26 March 2024; Accepted 3 April 2024
Available online 7 April 2024

consist of copper-based nanozymes (Liang et al., 2017; Tran et al., 2021; Song et al., 2023; Makam et al., 2022; Wang et al., 2019a, 2022a; Li et al., 2022), platinum-based nanozymes (Wang et al., 2017; Liu et al., 2015; Yang et al., 2023), gold-based nanozyme (Gugoasa et al., 2021), cerium based nanozyme (Liang et al., 2022), and lithium-based nanozymes (Wang et al., 2022b). Among them, researchers pay more attentions to Cu-based laccase mimetics than the others (Lei et al., 2022). We reason that there are two main reasons for this phenomenon: Firstly, natural laccase has a multi-copper center, thus using amino acids, nucleotides or organic small molecules to coordinate with Cu to construct biomimetic laccase-like nanozymes is more designed and rational than the trial-and-error strategy. Secondly, the prices of metals Pt, Au, and Li are much higher than Cu. However, for copper-based nanozymes, optimization of catalytic performance mainly focuses on screening and changing of ligands. There are few reports on improving activity by adjusting the composition of metal Cu. Since alloy-based catalysts have an easier-to-control electronic structure, better thermal stability and lower cost than single metal catalysts in catalytic reactions (Greeley and Mavrikakis, 2004; Tang et al., 2019; Fang et al., 2018). It is of great significance to use copper-based alloys to regulate the laccase-like activity of nanozymes.

Perovskite-based nanomaterials (oxides-ABO_3 or hydroxides-$AB(OH)_6$) have shown valuable applications in many fields due to their regular ReO_3 structure, easily controllable metal components (points A or B), and excellent catalytic properties (Peña and Fierro, 2001; Song et al., 2016; Fang et al., 2022; Hwang et al., 2017). Recently, perovskite-based nanozymes have also attracted much attentions, for example, Wei group has constructed some perovskite-based nanozymes via two strategies, one is designing the *eg* electron orbit of the A point of perovskite oxide (Wang et al., 2019b), another is using perovskite oxide as the base to grow noble metal nanoparticles (Jiang et al., 2021). Compared with perovskite oxides, perovskite hydroxides are another type of compounds with ReO_3 related structures. Their synthesis method (co-precipitation) is milder and simpler, and they are suitable as templates for multi-metal doping (Chen et al., 2018; Gao et al., 2018; Wu et al., 2022). In particular, the A point of perovskite hydroxide can be doped not only with various metals like Fe, Mn, Cu, Zn, and Ni but also alloys with two or more components can be synthesized. This characteristic permits the formation of diverse copper-containing alloys, which is advantageous for regulating the laccase-like activity of copper-containing alloys constructed from different combinations of metals and copper. Encouraged by this, it is reasonable and feasible to study the relationship between laccase-like activity and Cu-based alloys through regulating the A-point metal-doping in perovskite hydroxides.

Herein, as shown in Scheme 1, we selected perovskite hydroxide $AB(OH)_6$ as a model and successfully synthesized $CuSn(OH)_6$ nanozyme with laccase-like activity. Subsequently, we screened the A-point of $CuSn(OH)_6$ nanozyme via using Mn, a cheaper metal than copper, to construct alloys with Cu. Five binary perovskite hydroxide nanozymes ($Cu_{0.2}Mn_{0.8}Sn(OH)_6$, $Cu_{0.4}Mn_{0.6}Sn(OH)_6$, $Cu_{0.5}Mn_{0.5}Sn(OH)_6$, $Cu_{0.6}Mn_{0.4}Sn(OH)_6$, and $Cu_{0.8}Mn_{0.2}Sn(OH)_6$) with different Cu/Mn ratios were successfully synthesized. To our surprise, Cu/Mn alloy ratios of 0.5/0.5 and 0.8/0.2 can indeed enhance the laccase activity of $CuSn(OH)_6$. X-ray photoelectron spectroscopy (XPS) and inductively coupled plasma mass spectrometry (ICP-MS) results indicate that this increase in activity may be attributed to the Cu content and the Cu^{+}/Cu^{2+} ratio. Kinetic studies showed that this nanozyme has better catalytic efficiency than natural laccase. Furthermore, these nanozymes maintain excellent laccase-like activity at high temperatures and high ionic strengths. Finally, two types of substrates, toxic pollutants and catechol neurotransmitters, were used to react with these nanozymes. The results proved that these synthetic nanozymes have excellent environmental

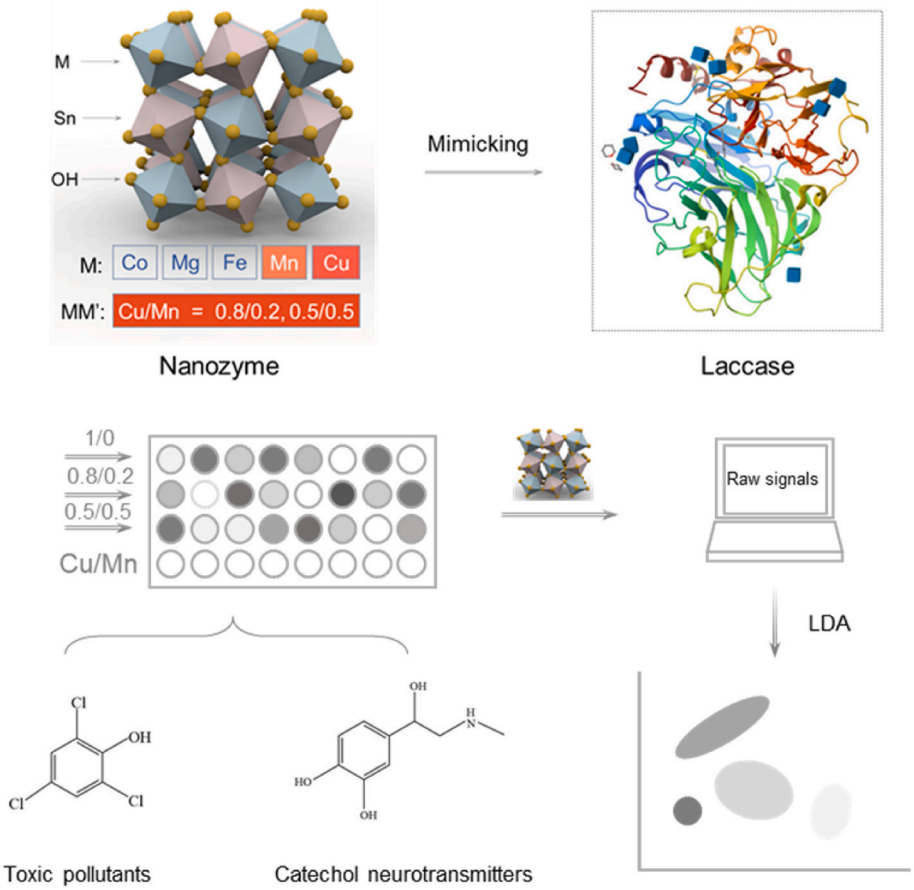

Scheme 1. Schematic illustration of the design of perovskite hydroxide-based laccase mimics for discriminating toxic pollutants and catechol neurotransmitters.

protection functions and biological detection properties.

2. Experimental

2.1. Synthesis of $MSn(OH)_6$

Typically, perovskite hydroxide $MSn(OH)_6$ was synthesized by a co-precipitation method according to previous literature with some modifications (Gao et al., 2018). Solution A: $CuSO_4{\cdot}5H_2O$ (2 mmol) and sodium citrate (2 mmol) were dissolved in 70 mL deionized water. Solution B: 2 mmol $SnCl_4{\cdot}5H_2O$ was dissolved in 10 mL ethanol. Then, solution B and solution A were mixed and stirred for 30 min. Subsequently, 10 mL of 2 M NaOH was added to the mixed solution in an 80 °C water bath. After 1 h, the precipitate was collected by centrifugation, washed several times with ethanol and deionized water, and dried at 60 °C. The synthesis of perovskite hydroxides for other metals (Co, Mg, Fe, Mn) is the same as above.

2.2. Synthesis of $MM'Sn(OH)_6$

The mixed metal perovskite hydroxides $MM'Sn(OH)_6$ were synthesized by the same method according to $MSn(OH)_6$. The difference is that the single metal M is replaced by alloy MM' with different proportions. For example, the solution A of $Cu_{0.5}Mn_{0.5}Sn(OH)_6$ is consist of $CuSO_4{\cdot}5H_2O$ (1 mmol), $(CH_3COO)_2Mn{\cdot}4H_2O$ (1 mmol) and sodium citrate (2 mmol). The following steps are the same as for $CuSn(OH)_6$ synthesis.

2.3. Measurement of the laccase-like activity

The laccase-like activity test of nanozymes was based on previous reports (Makam et al., 2022). First, 4-AP (0.5 mM) and 2,4-DP (0.6 mM) solutions were mixed with PBS buffer (pH 7.2). Next, nanozymes (0.1 mg/mL) was added. Then, the reaction system was incubated at 25 °C for 1 h, and then the reaction solution was transferred to a 96-well plate, and the absorbance value at 510 nm was measured using a microplate reader.

2.4. Kinetics assays

Various concentrations of 2,4-DP (0.1, 0.2, 0.3, 0.4, 0.5, 0.7, 1, 2 and 5 mM) were reacted with 0.5 mM 4-AP and 0.1 mg/mL nanozyme, respectively. Michaelis–Menten equation ($V_0 = V_{max}$ [S]/(K_M + [S]) was applied to obtain the kinetic parameters V_{max} and K_M. $k_{cat} = V_{max}$/[E]. [E] is the enzyme or nanozyme concentration. The molar concentration of the nanozyme was determined by a nanoparticle tracking analysis (NTA) system. First, measure the number of particles per milliliter with the NTA instrument, and then divide it by Avogadro's constant to get [E]. All measurements were replicated at least three times and averaged for accuracy.

2.5. Detoxify of toxic pollutants

Toxic pollutant (0.6 mM) was reacted with 0.5 mM 4-AP in PBS buffer (pH 7.2) containing 0.1 mg/mL nanozyme for 1 h at 25 °C. The color changing is recorded at the corresponding absorbance of 510 nm.

2.6. Discrimination of toxic pollutants

Eight kinds of toxic phenolic pollutants were detected as follows. PBS buffer (pH 7.2) containing nanozyme (100 μg/mL) and different concentration of analytes were incubated for 1 h at 25 °C. Then, 100 μL of each sample was added to a 96-well plate to collect absorbance. The eight toxic phenolic pollutants were tested against three nanozymes five times to give an eight toxic phenolic pollutants × three arrays × five replicates training data matrix. The raw data matrix was processed using Linear Discriminant Analysis (LDA).

2.7. Detection of epinephrine

Nanozyme (0.1 mg/mL) and epinephrine (0.5 mM) were mixed with PBS buffer (pH 7.2) for 1 h at 25 °C. The absorbance at 485 nm was collected. L-DOPA, dopamine, and norepinephrine were reacting following a similar process to that for epinephrine. To evaluate the detection limit of epinephrine, different concentrations of epinephrine (10, 20, 30, 40, 50, 60, 80, 100, 150, 200, and 300 μM) were mixed with 0.1 mg/mL nanozyme in the PBS buffer for 1 h at 25 °C. The detection limit was calculated by 3σ/b, where σ is the standard deviation of the blank signals, and b is the slope of the regression line.

2.8. Discrimination of catecholamine neurotransmitters

PBS buffer (pH 7.2) containing nanozyme (100 μg/mL) and different concentration of substrate was incubated for 1 h at 25 °C. Then, 100 μL of each sample was added to a 96-well plate to collect absorbance. The four catecholamine neurotransmitters were tested against three nanozymes five times to give a four catecholamine neurotransmitters × three arrays × five replicates training data matrix. The raw data matrix was processed using Linear Discriminant Analysis (LDA).

2.9. Measurements of Cu and Mn contents

The amounts of Cu and Mn in $CuSn(OH)_6$, $Cu_{0.5}Mn_{0.5}Sn(OH)_6$ and $Cu_{0.8}Mn_{0.2}Sn(OH)_6$ were analyzed by ICP-MS (Agilent 7700, USA). Before measurements, $CuSn(OH)_6$, $Cu_{0.5}Mn_{0.5}Sn(OH)_6$ and $Cu_{0.8}Mn_{0.2}Sn(OH)_6$ were first digested at aqua regia overnight respectively, and diluted with water.

3. Results and discussion

3.1. Exploring perovskite hydroxide $MSn(OH)_6$ with laccase-like activity

Perovskite hydroxides are compounds with a typical ReO_3-related structure (Fig. 1A) (Evans et al., 2020). Here, five perovskite hydroxides with $MSn(OH)_6$ (M = Co, Mg, Fe, Mn, and Cu) structures were synthesized using a simple co-precipitation method. Scanning electron microscopy (SEM) showed their cubic morphology with dimensions ranging from 50 to 450 nm (Fig. 1B and Fig. S1). Meanwhile, the powder X-ray diffraction (PXRD) spectra showed that these $MSn(OH)_6$ are consistent with a previous report (Wu et al., 2022) (Fig. 1C).

As shown in Fig. 1D, the laccase-mimicking activity of these perovskite hydroxides was evaluated by the typical color changing reaction of 2,4-dichlorophenol (2,4-DP) with 4-aminoantipyrine (4-AP). We found that 2,4-DP reacts with 4-AP only in the presence of $CuSn(OH)_6$, producing a wine-red product with a characteristic UV-visible absorption peak at 510 nm, which indicates that $CuSn(OH)_6$ has excellent laccase-like activity. Subsequently, we tested four other perovskite hydroxides using the same method and compared their activity with $CuSn(OH)_6$. The results show that among these perovskite hydroxides, only when Cu occupies A-site, it has excellent laccase-like catalytic activity, which is consistent with the catalytic center of natural laccase being metal Cu (Fig. 1E and Fig. S3).

3.2. Exploring perovskite hydroxide $MM'Sn(OH)_6$ with laccase-like activity

In the $AB(OH)_6$ structure of perovskite hydroxide, the metal A-site can be occupied by mixed metals. Very recently, perovskite hydroxides with high-entropy alloys occupying the A-site were successfully synthesized (Wu et al., 2022). Inspired by this, we selected metal Mn, which also has the laccase-like activity when occupied A-site in the $AB(OH)_6$ structure, to mix with Cu to synthesize binary alloy perovskites

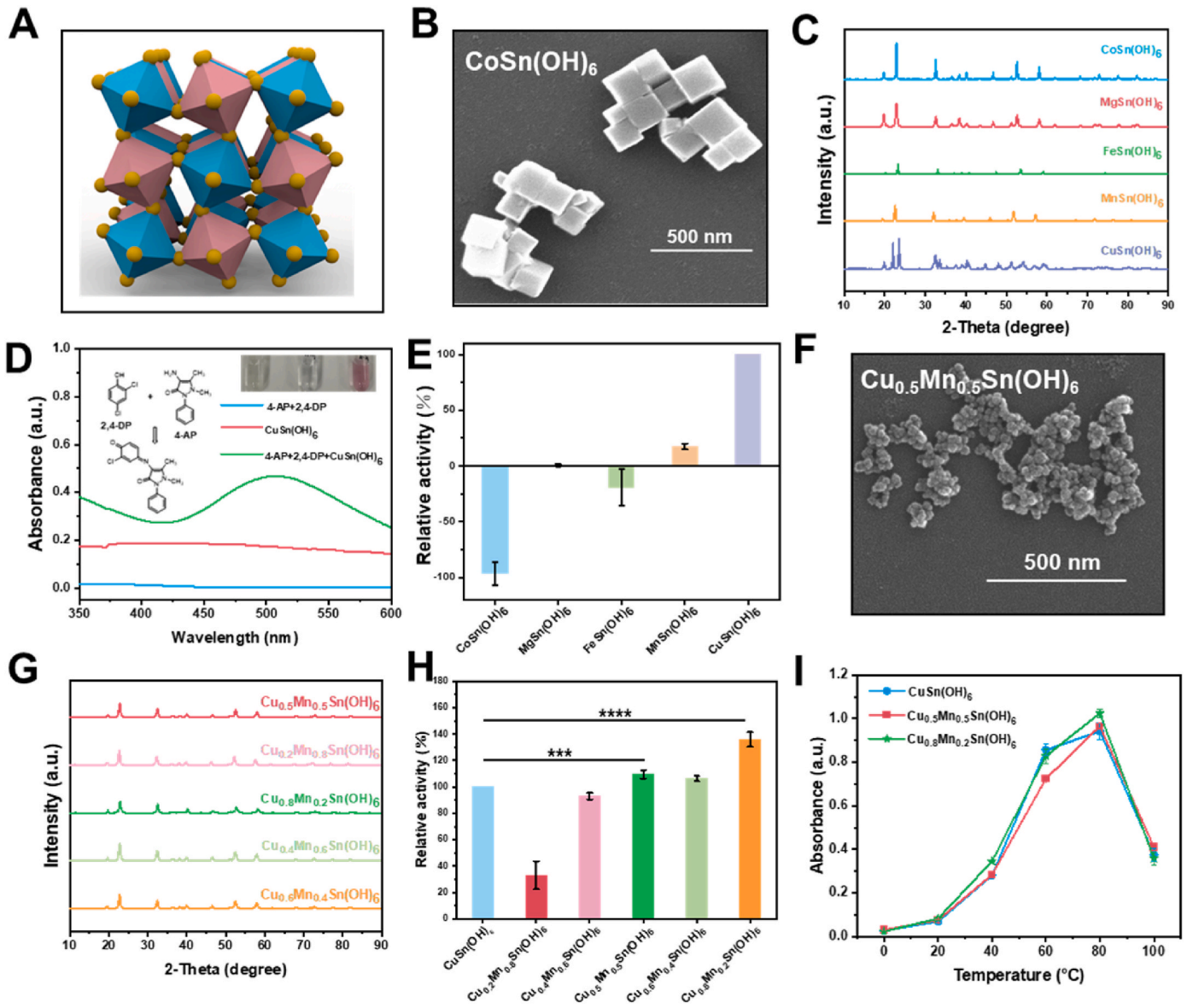

Fig. 1. (A) Schematic diagram of the perovskite hydroxide structure. (B) SEM image of $CoSn(OH)_6$. (C) PXRD patterns of $CoSn(OH)_6$, $MgSn(OH)_6$, $FeSn(OH)_6$, $MnSn(OH)_6$, and $CuSn(OH)_6$. (D) Laccase-like activity measurement of $CuSn(OH)_6$. Inset: Typical reaction for evaluating the laccase-like activities, photograph of the corresponding samples. (E) Relative laccase-like activity of five perovskite hydroxides, the laccase-like activity of $CuSn(OH)_6$ was set as 100%. (F) SEM image of $Cu_{0.5}Mn_{0.5}Sn(OH)_6$. (G) PXRD patterns of $Cu_{0.5}Mn_{0.5}Sn(OH)_6$, $Cu_{0.2}Mn_{0.8}Sn(OH)_6$, $Cu_{0.8}Mn_{0.2}Sn(OH)_6$, $Cu_{0.4}Mn_{0.6}Sn(OH)_6$, and $Cu_{0.6}Mn_{0.4}Sn(OH)_6$. (H) Relative laccase-like activity of binary alloy perovskite hydroxides, the laccase-like activity of $CuSn(OH)_6$ was set as 100%. (I) Relative activity of $CuSn(OH)_6$, $Cu_{0.5}Mn_{0.5}Sn(OH)_6$, and $Cu_{0.8}Mn_{0.2}Sn(OH)_6$ under different temperatures. Error bars in all figures mean standard deviations of 3 independent tests.

hydroxides with different ratios of Cu/Mn. As shown in Fig. 1F and Fig. S2, SEM images indicated that binary $CuMnSn(OH)_6$ compounds with Cu/Mn ratios of 0.2/0.8, 0.4/0.6, 0.5/0.5, 0.6/0.4, and 0.8/0.2 still have cubic morphology. But compared to $CuSn(OH)_6$, the size of the binary material is significantly smaller, around 30–100 nm. PXRD spectra exhibited that these binary alloy perovskite hydroxides also have typical perovskites hydroxide structures (Fig. 1G). To further demonstrate the success synthesis of Mn/Cu alloy, SEM element mapping tests were conducted on $CuSn(OH)_6$, $Cu_{0.5}Mn_{0.5}Sn(OH)_6$, and $Cu_{0.8}Mn_{0.2}Sn(OH)_6$. The results also proved that the two Mn and Cu elements do exist in such binary alloy perovskites hydroxides (Fig. S6-Fig. S11).

Then, we tested the laccase-like activity of these five binary alloy perovskite hydroxides. As shown in Fig. 1H, using $CuSn(OH)_6$ as reference, we found that the ratio of Cu and Mn has a significant impact on the laccase-like activity of these perovskite hydroxides. Specifically, the laccase-like activities of $Cu_{0.5}Mn_{0.5}Sn(OH)_6$, $Cu_{0.6}Mn_{0.4}Sn(OH)_6$ and $Cu_{0.8}Mn_{0.2}Sn(OH)_6$ were higher than those of the reference, and $Cu_{0.8}Mn_{0.2}Sn(OH)_6$ has the highest activity. At the same time, the laccase-like activities of $Cu_{0.4}Mn_{0.6}Sn(OH)_6$ and $Cu_{0.2}Mn_{0.8}Sn(OH)_6$ were lower than those of the reference, and $Cu_{0.2}Mn_{0.8}Sn(OH)_6$ has the lowest activity. These results show that: (1) When the Cu/Mn ratio is greater than 1, the higher the ratio, the stronger the activity, which is higher than the reference; (2) When the Cu/Mn ratio is 1, the activity is slightly higher than the reference; (3) When the Cu/Mn ratio is less than 1, its activity is lower than the reference and the lower the ratio, the lower the activity. Moreover, we have synthesized alloys containing between three to seven elements (Fig. S22). However, in testing their laccase-like activity, we found that except for the binary CuMn alloy, other multi-component alloys could not provide outstanding catalytic performance.

3.3. Mechanism study

To explore the mechanism of the above-mentioned differences in laccase-like activity, ICP-MS and XPS were used to evaluate $CuSn(OH)_6$, $Cu_{0.5}Mn_{0.5}Sn(OH)_6$ and $Cu_{0.8}Mn_{0.2}Sn(OH)_6$. First, at the same mass concentration, the ICP-MS results showed that the Cu contents in $CuSn(OH)_6$, $Cu_{0.5}Mn_{0.5}Sn(OH)_6$ and $Cu_{0.8}Mn_{0.2}Sn(OH)_6$ are 30%, 11% and 17%, and the Sn contents are 28%, 34% and 33%. Meanwhile, the Mn contents in $Cu_{0.5}Mn_{0.5}Sn(OH)_6$ and $Cu_{0.8}Mn_{0.2}Sn(OH)_6$ are 10% and 6%. In addition, we have measured the Brunauer-Emmett-Teller (BET) surface areas of $CuSn(OH)_6$ (36.01 m^2g^{-1}), $Cu_{0.5}Sn_{0.5}(OH)_6$ (65.86 m^2g^{-1}) and $Cu_{0.8}Sn_{0.2}(OH)_6$ (36.08 m^2g^{-1}) (Fig. S20 and Table S3). Since Cu is the active site of natural laccase and most laccase-like mimics, its content should theoretically be positively correlated with laccase-like activity. However, we found that after incorporating Mn into $CuSn(OH)_6$, although the contents of Cu obviously decreased, the activities of the Cu/Mn alloy perovskite hydroxides $Cu_{0.5}Mn_{0.5}Sn(OH)_6$ and $Cu_{0.8}Mn_{0.2}Sn(OH)_6$ were still higher than that of the single Cu activity. It demonstrates that when the copper content is low, the specific surface area plays an important role in enhancing its catalytic activity. We then ran XPS tests on these materials. The survey spectra, O 1s, Sn 3 d, and Mn 2p were shown in Fig. S12, Fig. S13, and Fig. S14. The spectra of Cu 2p showed that the ratios of Cu^+/Cu^{2+} are different among $CuSn(OH)_6$, $Cu_{0.5}Mn_{0.5}Sn(OH)_6$ and $Cu_{0.8}Mn_{0.2}Sn(OH)_6$. As shown in Fig. 2, doping Mn element can increase the ratio of Cu^+/Cu^{2+} from 13/87 to 26/74. We deduced that the increased proportion of Cu^+ may also be responsible for the increased activity.

To further optimize the catalytic activity, we selected $CuSn(OH)_6$, $Cu_{0.5}Mn_{0.5}Sn(OH)_6$ and $Cu_{0.8}Mn_{0.2}Sn(OH)_6$ with higher laccase-like activity to test their activities under different temperatures and ionic strengths. As shown in Fig. 1I–as the temperature increases, these three nanozymes all showed enhanced activity, and their optimal reaction temperatures are all 80 °C. We then used NaCl to change the ionic strength of the solution. As the concentration of NaCl increased, $Cu_{0.8}Mn_{0.2}Sn(OH)_6$ still had the optimal activity among all three materials (Fig. S4). Besides, we investigated how pH impacts the laccase-like activity of perovskite hydroxide nanozymes. As shown in Fig. S19A, the optimal pH value for the laccase-like activity of $CuSn(OH)_6$, $Cu_{0.5}Mn_{0.5}Sn(OH)_6$, and $Cu_{0.8}Mn_{0.2}Sn(OH)_6$ is 7. At the same time, the optimal pH value of $Cu_{0.8}Mn_{0.2}Sn(OH)_6$ for eight different substrates is also 7 (Fig. S19B). Furthermore, the stability and recyclability of these nanozymes were evaluated with good results showing their effective performances (Figs. S21 and S24).

3.4. Kinetic study

In addition, the typical Michaelis–Menten curves were obtained and kinetic parameters were calculated based on the equation: $V = V_{max}[S]/(K_m + [S])$, where V is the initial velocity, $[S]$ is the concentration of substrate, V_{max} is the maximum reaction velocity, and K_m is the Michaelis constant. As shown in Fig. S5 and Table S1, the catalytic efficiency ($k_{cat}/K_m = 3.37 \times 10^5$ mM^{-1} s^{-1}) and the maximum reaction velocity ($V_{max} = 3.25 \times 10^{-5}$ mM^{-1} s^{-1}) of $Cu_{0.5}Mn_{0.5}Sn(OH)_6$ are much higher than that of $CuSn(OH)_6$ and $Cu_{0.8}Mn_{0.2}Sn(OH)_6$. It is worth mentioning that the k_{cat}/K_m values of our synthesized laccase-like mimetics are much higher than that of natural laccase (Makam et al., 2022) (Fig. S18 and Table S1).

3.5. Discrimination and detoxify of environmental toxic pollutants

Distinguishing and degrading different environmental pollutants can not only improve the efficiency of environmental protection, but also help analyze the composition of polluted water, trace the source of pollution, and solve environmental problems further upstream. Although laccase and its mimetics exhibited excellent degradation of toxic phenolic pollutants, there are still relatively few studies distinguishing the pollutants. Here, three nanozymes ($CuSn(OH)_6$, $Cu_{0.5}Mn_{0.5}Sn(OH)_6$ and $Cu_{0.8}Mn_{0.2}Sn(OH)_6$) with laccase-like activity were used to construct a sensor array for distinguishing eight toxic pollutants (Fig. 3A and B). Fig. 3C ~ Fig. 3E and Fig. S15 showed that these three nanozymes can catalyze the oxidation of all eight pollutants and make them show different colors. Linear discriminant analysis (LDA) is a supervised learning technique that aims to maximize the separation between classes by finding projection vectors. It does so by separating samples from different categories while clustering together samples from the same category to enable classification. In areas like analysis and detection, LDA is commonly utilized to reduce the dimensionality of intricate high-dimensional data and isolate its key characteristics. Thus, analyzing these signals by LDA could convert the training matrix into three canonical scores, and the first two most important discriminating factors could generate 2D canonical score plots. To optimize the sensor array, we first fixed the concentration of the substrate to screen the optimal concentration of the nanozyme. Fig. S16 showed that when the concentration of these nanozymes is 0.05 mg/mL, the sensor array has the best discrimination effect for all pollutants. Subsequently, we applied this sensor array to distinguish eight contaminants at concentrations ranging from 0.4 to 1.0 mM. Fig. 3F ~ Fig. 3H showed the substrate discrimination effect of this sensor array, that is, when the substrate concentration is 0.4 and 0.6 mM, these eight substrates can be effectively distinguished; when the substrate concentration is increased to 1.0 mM, all contaminants cannot be completely distinguished.

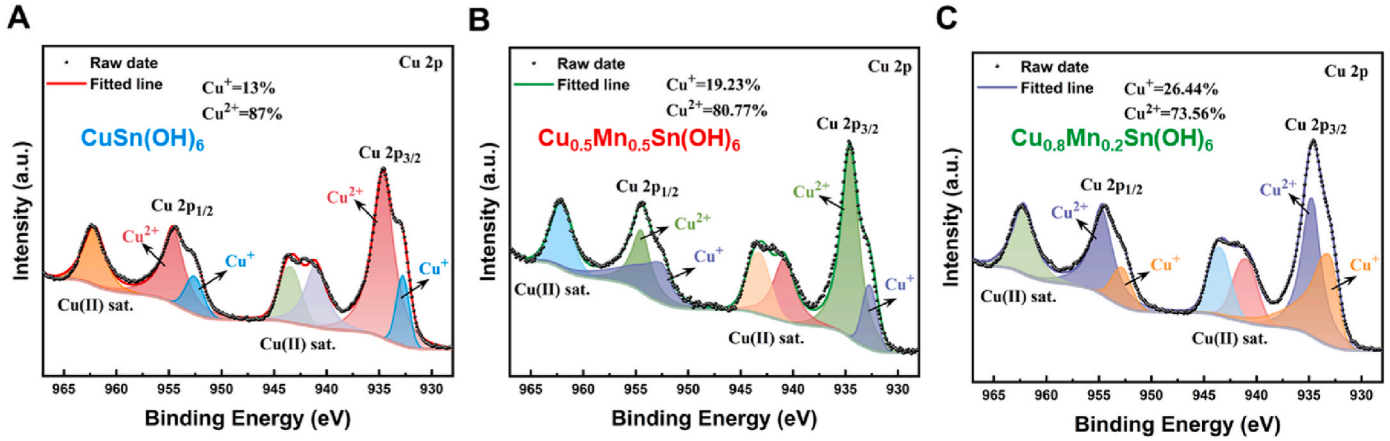

Fig. 2. The Cu 2p XPS spectra of (A) $CuSn(OH)_6$, (B) $Cu_{0.5}Mn_{0.5}Sn(OH)_6$, and (C) $Cu_{0.8}Mn_{0.2}Sn(OH)_6$.

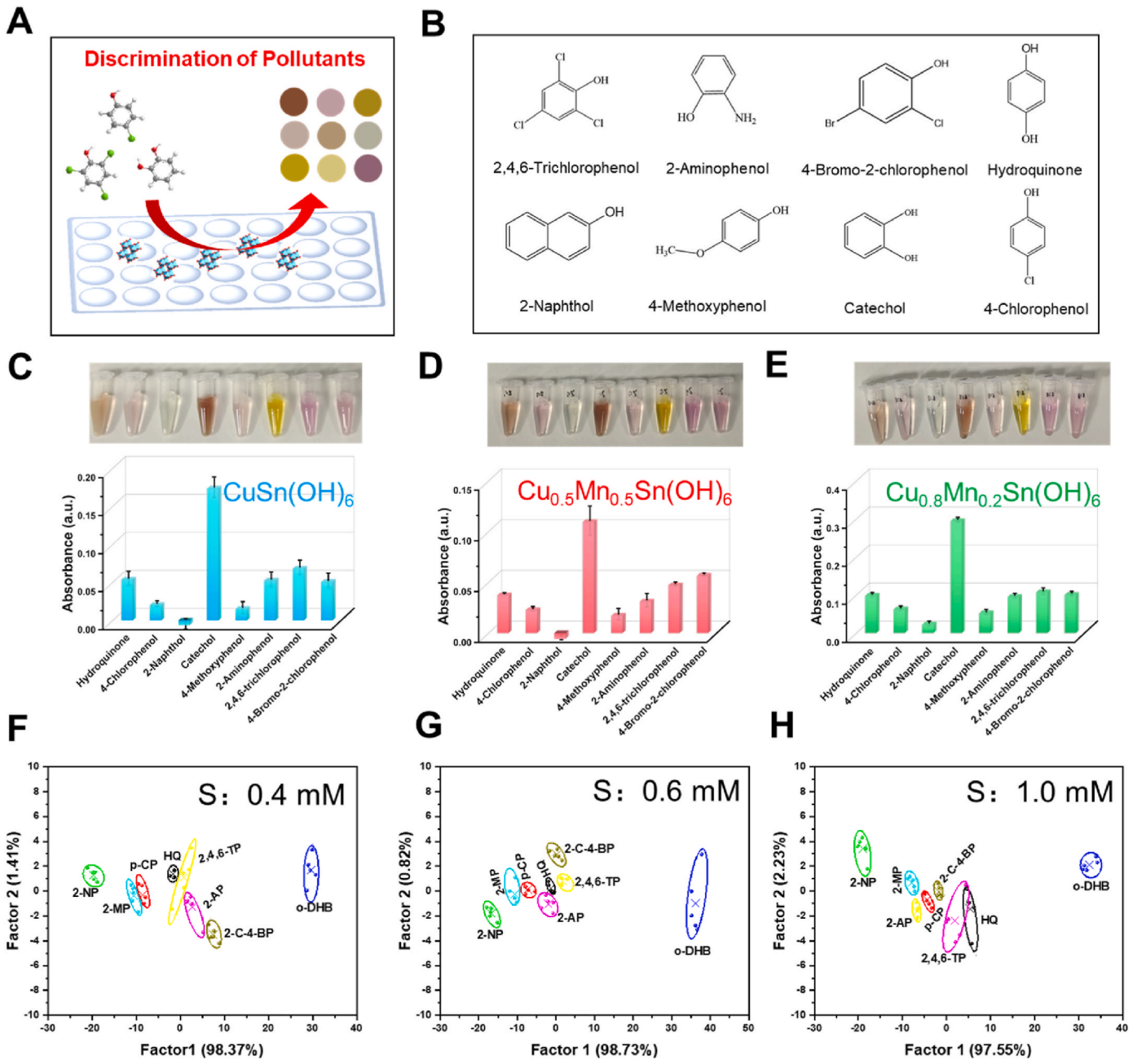

Fig. 3. (A) Schematic diagram of the discrimination of pollutants in the presence of the perovskite hydroxide-based sensor array. (B) Chemical formulas of 8 toxic pollutants. Absorbance of 8 pollutants in the presence of (C) $CuSn(OH)_6$, (D) $Cu_{0.5}Mn_{0.5}Sn(OH)_6$, and (E) $Cu_{0.8}Mn_{0.2}Sn(OH)_6$. Photographs represent corresponding samples. Sensor arrays for discriminations against pollutants in (F) 0.4 mM, (G) 0.6 mM, and (H) 1.0 mM. Error bars in all figures mean standard deviations of 3 independent tests.

3.6. Colorimetric detection and identification of catecholamine neurotransmitters

Catecholamines are hormones produced by the brain, nervous tissue, and adrenal glands, including dopamine (DA), epinephrine (EP), Levodopa (LD), and norepinephrine (NE). They are substances released by the body in response to emotions or physiology pressure. Abnormal catecholamine levels may indicate a serious underlying disease. Therefore, highly sensitive detection and differentiation of multiple catecholamines is needed. Since catecholamine neurotransmitters are another phenolic substrate, nanozymes with laccase-like activity can react with them to produce colored products. Thus, we applied $CuSn(OH)_6$, $Cu_{0.5}Mn_{0.5}Sn(OH)_6$ and $Cu_{0.8}Mn_{0.2}Sn(OH)_6$ as functional colorimetric probes to detect catecholamines.

Epinephrine, a typical catecholamine neurotransmitter, was selected for detection. As depicted in Fig. 4A–B, Fig. 4D–E, Fig. 4G, and Fig. 4H, the characteristic UV-vis absorbances of oxidized EP gradually increased with enhancing the EP concentrations from 10 to 300 μM, indicating the excellent detectability of $CuSn(OH)_6$, $Cu_{0.5}Mn_{0.5}Sn(OH)_6$ and $Cu_{0.8}Mn_{0.2}Sn(OH)_6$ toward EP. In addition, Fig. 4C–F, Fig. 4I, and Table S2 showed linear relationships between the absorbances at 485 nm and EP concentrations in the ranges from 50 to 150 μM ($CuSn(OH)_6$), 20–200 μM ($Cu_{0.5}Mn_{0.5}Sn(OH)_6$), and 10–150 μM ($Cu_{0.8}Mn_{0.2}Sn(OH)_6$), respectively. The detection limits of $CuSn(OH)_6$, $Cu_{0.5}Mn_{0.5}Sn(OH)_6$ and $Cu_{0.8}Mn_{0.2}Sn(OH)_6$ were 14.6, 9.3, and 3.5 μM respectively, indicating that the $Cu_{0.8}Mn_{0.2}Sn(OH)_6$ probe has the highest sensitivity for EP

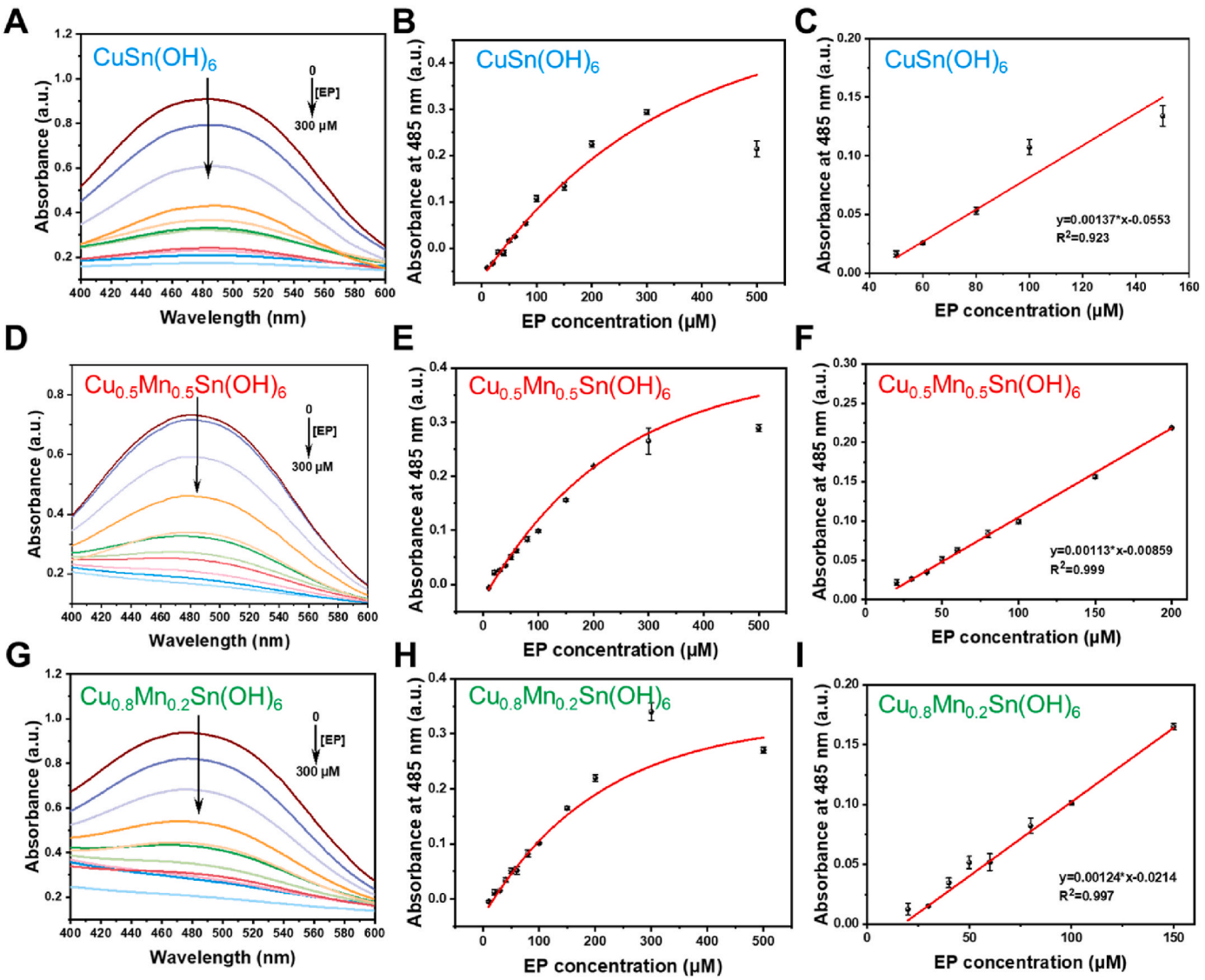

Fig. 4. (A)(D)(G) UV-visible absorption spectra of $CuSn(OH)_6$, $Cu_{0.5}Mn_{0.5}Sn(OH)_6$, and $Cu_{0.8}Mn_{0.2}Sn(OH)_6$ catalyzed 4-AP and 2,4-DP in the presence of EP with different concentrations, respectively. (B)(E)(H) Panel A, D and G, absorbance at 485 nm versus EP concentration. (C)(F)(I) Panel A, D and G, the linear calibration plotted in the concentration range from 50 to 150 μM, 20–200 μM, and 20–150 μM, respectively. Error bars in all figures mean standard deviations of 3 independent tests.

biosensing.

Then, three nanozymes ($CuSn(OH)_6$, $Cu_{0.5}Mn_{0.5}Sn(OH)_6$ and $Cu_{0.8}Mn_{0.2}Sn(OH)_6$) with laccase mimicking activities were applied to construct a sensor array for discrimination of EP, NE, DA, and LD (Fig. 5A). As shown in Fig. 5B ~ Fig. 5D, these four neurotransmitters showed different signals on the sensor array. We found that sensor arrays with nanozymes at concentrations of 0.05, 0.10, 0.20, and 0.50 mg/mL could completely distinguish these four neurotransmitters (Fig. S17). We then used the sensor array constructed with the lowest concentration of nanozyme (0.05 mg/mL) to distinguish different concentrations of neurotransmitters. Fig. 5E and F showed that this sensor array can completely distinguish neurotransmitters at concentrations of 0.2 and 0.8 mM.

4. Conclusions

In summary, we have developed the perovskite hydroxides-based nanozymes with excellent laccase-like activity. We found that introducing alloys with different "Cu/Mn" ratios into the A-site of the perovskite hydroxide structure can modulate its laccase-like activity. Through XPS and ICP-MS measurements, we infer that the regulation of laccase activity of these nanozymes is mainly attributed to the ratio of Cu^{+}/Cu^{2+} and Cu content. Moreover, we found that these laccase-like nanozymes could not only efficiently detoxify toxic pollutants but also had highly sensitive detection capabilities for neurotransmitter. Benefiting from such functions, a sensor array using three nanozymes of $CuSn(OH)_6$, $Cu_{0.5}Mn_{0.5}Sn(OH)_6$ and $Cu_{0.8}Mn_{0.2}Sn(OH)_6$ was established and successfully applied to distinguish eight different pollutants and four different neurotransmitters, respectively. We hope that this work will encourage more researchers to develop laccase-like nanozymes with low price and superior activity, and further apply them in a wider range of environmental and biomedical fields.

CRediT authorship contribution statement

Yufeng Liu: Writing – review & editing, Writing – original draft, Data curation, Conceptualization. **Jing Zhang:** Writing – review & editing, Writing – original draft, Data curation. **Shuai Cui:** Writing – review & editing, Data curation. **Hui Wei:** Writing – review & editing, Writing – original draft, Conceptualization. **Dongzhi Yang:** Writing –

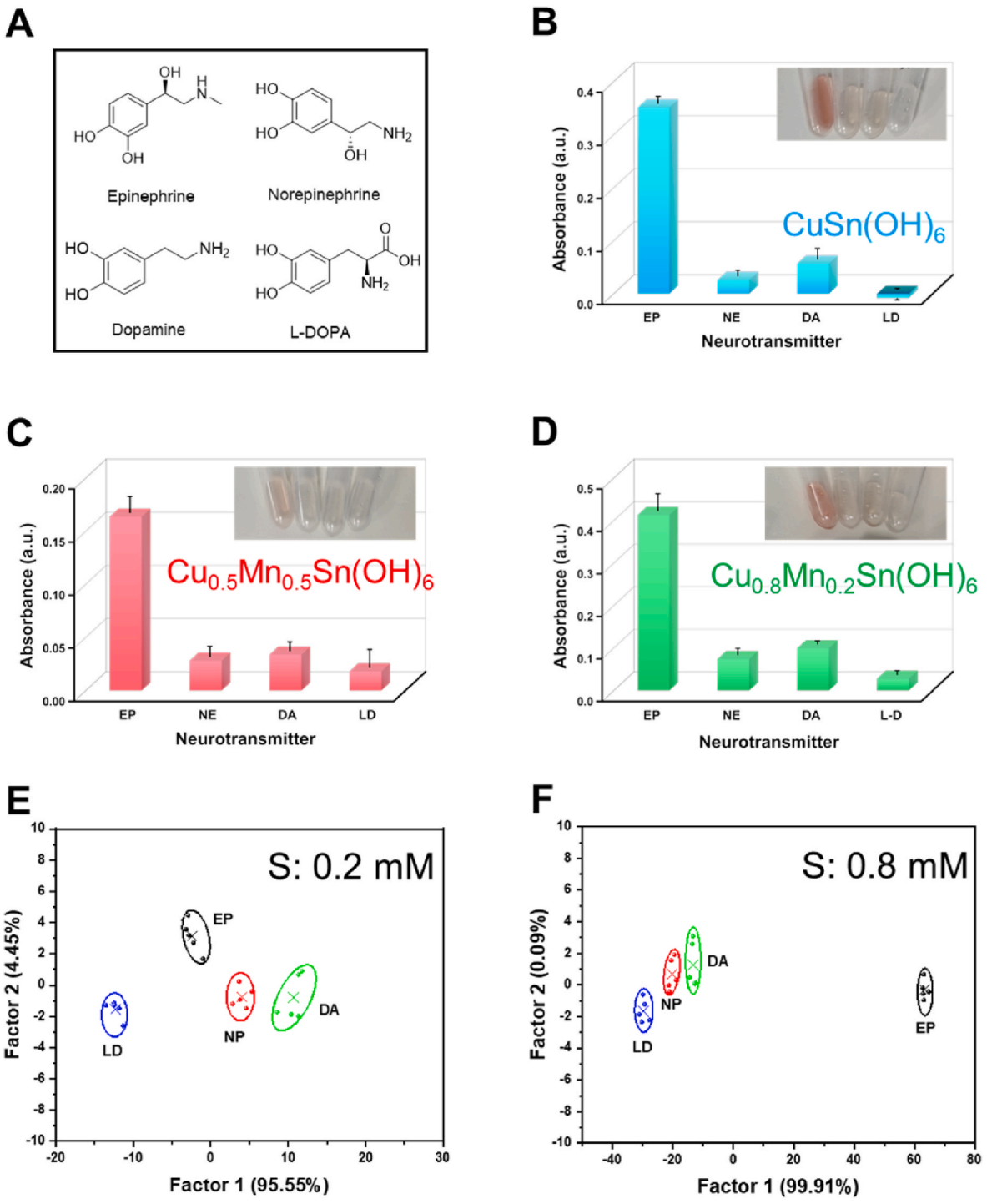

Fig. 5. (A) Chemical formulas of epinephrine, norepinephrine, dopamine, and L-dopa. Absorbance of four kinds of catecholamine neurotransmitters in the presence of (B) $CuSn(OH)_6$, (C) $Cu_{0.5}Mn_{0.5}Sn(OH)_6$, and (D) $Cu_{0.8}Mn_{0.2}Sn(OH)_6$. Photographs represent corresponding samples. Sensor arrays for discriminations against catecholamine neurotransmitters in (E) 0.2 mM and (F) 0.8 mM. Error bars in all figures mean standard deviations of 3 independent tests.

review & editing, Writing – original draft, Conceptualization.

Declaration of competing interest

The authors declare that they have no conflict of interest.

Data availability

Data will be made available on request.

Acknowledgements

This work was supported by National Natural Science Foundation of China (22307110), the Natural Science Research General Project of Jiangsu Province Colleges and Universities (23KJD150009). Xuzhou Medical University scientific research funding (D2022057).

Appendix A. Supplementary data

Supplementary data to this article can be found online at https://doi.org/10.1016/j.bios.2024.116275.

References

Chen, Z., Yin, J.-J., Zhou, Y.-T., Zhang, Y., Song, L., Song, M., Hu, S., Gu, N., 2012. Dual enzyme-like activities of iron oxide nanoparticles and their implication for diminishing cytotoxicity. ACS Nano 6 (5), 4001–4012. https://doi.org/10.1021/nn300291r.

Chen, D., Qiao, M., Lu, Y.R., Hao, L., Liu, D., Dong, C.L., Li, Y., Wang, S., 2018. Preferential cation vacancies in perovskite hydroxide for the oxygen evolution reaction. Angew. Chem. Int. Ed. 57 (28), 8691–8696. https://doi.org/10.1002/anie.201805520.

Couto, S.R., Herrera, J.L.T., 2006. Industrial and biotechnological applications of laccases: a review. Biotechnol. Adv. 24 (5), 500–513. https://doi.org/10.1016/j.biotechadv.2006.04.003.

Cui, Z., Li, Y., Zhang, H., Qin, P., Hu, X., Wang, J., Wei, G., Chen, C., 2022. Lighting up agricultural sustainability in the new era through nanozymology: an overview of classifications and their agricultural applications. J. Agric. Food Chem. 70 (42), 13445–13463. https://doi.org/10.1021/acs.jafc.2c04882.

Dong, Z., Luo, Q., Liu, J., 2012. Artificial enzymes based on supramolecular scaffolds. Chem. Soc. Rev. 41 (23), 7890–7908. https://doi.org/10.1039/C2CS35207A.

Evans, H.A., Wu, Y., Seshadri, R., Cheetham, A.K., 2020. Perovskite-related ReO3-type structures. Nat. Rev. Mater. 5 (3), 196–213. https://doi.org/10.1038/s41578-019-0160-x.

Fang, H., Yang, J., Wen, M., Wu, Q., 2018. Nanoalloy materials for chemical catalysis. Adv. Mater. 30 (17), 1705698 https://doi.org/10.1002/adma.201705698.

Fang, Y., Fang, Y., Zong, R., Yu, Z., Tao, Y., Shao, J., 2022. In situ surface reconstruction of a Ni-based perovskite hydroxide catalyst for an efficient oxygen evolution reaction. J. Mater. Chem. A 10 (3), 1369–1379. https://doi.org/10.1039/D1TA08531J.

Fang, Q., Liu, Q., Zhang, Y., Du, Y., 2023. Fe3N-decorated porous carbon frameworks from wheat flour with dual enzyme-mimicking activities for organic pollutant degradation. Nanoscale 15 (22), 9718–9727. https://doi.org/10.1039/d3nr00048f.

Gao, L., Zhuang, J., Nie, L., Zhang, J., Zhang, Y., Gu, N., Wang, T., Feng, J., Yang, D., Perrett, S., Yan, X., 2007. Intrinsic peroxidase-like activity of ferromagnetic nanoparticles. Nat. Nanotechnol. 2 (9), 577–583. https://doi.org/10.1038/nnano.2007.260.

Gao, Y., Ye, L., Cao, S., Chen, H., Yao, Y., Jiang, J., Sun, L., 2018. Perovskite hydroxide CoSn (OH) 6 nanocubes for efficient photoreduction of CO2 to CO. ACS Sustain. Chem. Eng. 6 (1), 781–786. https://doi.org/10.1021/acssuschemeng.7b03119.

Greeley, J., Mavrikakis, M., 2004. Alloy catalysts designed from first principles. Nat. Mater. 3 (11), 810–815. https://doi.org/10.1038/nmat1223.

Gugoasa, L.A.D., Pogacean, F., Kurbanoglu, S., Tudoran, L.-B., Serban, A.B., Kacso, I., Pruneanu, S., 2021. Graphene-gold nanoparticles nanozyme-based electrochemical sensor with enhanced laccase-like activity for determination of phenolic substrates. J. Electrochem. Soc. 168 (6), 067523 https://doi.org/10.1149/1945-7111/ac0c32.

Han, J., Wang, J., Wang, J., Fan, D., Dong, S., 2022. Recent advancements in coralyne (COR)-based biosensors: basic principles, various strategies and future perspectives. Biosens. Bioelectron. 210 https://doi.org/10.1016/j.bios.2022.114343.

Hou, J., Wang, J., Han, J., Wang, J., Chao, D., Dong, Q., Fan, D., Dong, S., 2024. An intelligent ratiometric fluorescent assay based on MOF nanozyme-mediated tandem catalysis that guided by contrary logic circuit for highly sensitive sarcosine detection and smartphone-based portable sensing application. Biosens. Bioelectron. 249 https://doi.org/10.1016/j.bios.2024.116035.

Huang, Y., Ren, J., Qu, X., 2019a. Nanozymes: classification, catalytic mechanisms, activity regulation, and applications. Chem. Rev. 119 (6), 4357–4412. https://doi.org/10.1021/acs.chemrev.8b00672.

Huang, L., Chen, J., Gan, L., Wang, J., Dong, S., 2019b. Single-atom nanozymes. Sci. Adv. 5 (5), eaav5490 https://doi.org/10.1126/sciadv.aav5490.

Hwang, J., Rao, R.R., Giordano, L., Katayama, Y., Yu, Y., Shao-Horn, Y., 2017. Perovskites in catalysis and electrocatalysis. Science 358 (6364), 751–756. https://doi.org/10.1126/science.aam7092.

Jiang, D., Ni, D., Rosenkrans, Z.T., Huang, P., Yan, X., Cai, W., 2019. Nanozyme: new horizons for responsive biomedical applications. Chem. Soc. Rev. 48 (14), 3683–3704. https://doi.org/10.1039/C8CS00718G.

Jiang, X., Wang, X., Lin, A., Wei, H., 2021. In situ exsolution of noble-metal nanoparticles on perovskites as enhanced peroxidase mimics for bioanalysis. Anal. Chem. 93 (14), 5954–5962. https://doi.org/10.1021/acs.analchem.1c00721.

Lei, L., Yang, X., Song, Y., Huang, H., Li, Y., 2022. Current research progress on laccase-like nanomaterials. New J. Chem. 46 (8), 3541–3550. https://doi.org/10.1039/D1NJ05658A.

Li, X., Wang, L., Du, D., Ni, L., Pan, J., Niu, X., 2019. Emerging applications of nanozymes in environmental analysis: opportunities and trends. Trends Analyt. Chem. 120, 115653 https://doi.org/10.1016/j.trac.2019.115653.

Li, S., Zhang, Y., Wang, Q., Lin, A., Wei, H., 2021. Nanozyme-enabled analytical chemistry. Anal. Chem. 94 (1), 312–323. https://doi.org/10.1021/acs.analchem.1c04492.

Li, M., Xie, Y., Lei, L., Huang, H., Li, Y., 2022. Colorimetric logic gate for protamine and trypsin based on the Bpy-Cu nanozyme with laccase-like activity. Sens. Actuators B Chem. 357, 131429 https://doi.org/10.1016/j.snb.2022.131429.

Liang, H., Lin, F., Zhang, Z., Liu, B., Jiang, S., Yuan, Q., Liu, J., 2017. Multicopper laccase mimicking nanozymes with nucleotides as ligands. ACS Appl. Mater. Interfaces 9 (2), 1352–1360. https://doi.org/10.1021/acsami.6b15124.

Liang, S., Wu, X.-L., Xiong, J., Yuan, X., Liu, S.-L., Zong, M.-H., Lou, W.-Y., 2022. Multivalent Ce-MOFs as biomimetic laccase nanozyme for environmental remediation. Chem. Eng. J. 450, 138220 https://doi.org/10.1016/j.cej.2022.138220.

Liu, Y., Wu, H., Chong, Y., Wamer, W.G., Xia, Q., Cai, L., Nie, Z., Fu, P.P., Yin, J.-J., 2015. Platinum nanoparticles: efficient and stable catechol oxidase mimetics. ACS Appl. Mater. Interfaces 7 (35), 19709–19717. https://doi.org/10.1021/acsami.5b05180.

Liu, X., Huang, D., Lai, C., Zeng, G., Qin, L., Wang, H., Yi, H., Li, B., Liu, S., Zhang, M., 2019. Recent advances in covalent organic frameworks (COFs) as a smart sensing material. Chem. Soc. Rev. 48 (20), 5266–5302. https://doi.org/10.1039/C9CS00299E.

Ma, L., Zheng, J.-J., Zhou, N., Zhang, R., Fang, L., Yang, Y., Gao, X., Chen, C., Yan, X., Fan, K., 2024. A natural biogenic nanozyme for scavenging superoxide radicals. Nat. Commun. 15 (1) https://doi.org/10.1038/s41467-023-44463-w.

Makam, P., Yamijala, S.S., Bhadram, V.S., Shimon, L.J., Wong, B.M., Gazit, E., 2022. Single amino acid bionanozyme for environmental remediation. Nat. Commun. 13 (1), 1505. https://doi.org/10.1038/s41467-022-28942-0.

Mayer, A.M., Staples, R.C., 2002. Laccase: new functions for an old enzyme. Phytochemistry 60 (6), 551–565. https://doi.org/10.1016/S0031-9422(02)00171-1.

Meng, Y., Li, W., Pan, X., Gadd, G.M., 2020. Applications of nanozymes in the environment. Environ. Sci.: Nano 7 (5), 1305–1318. https://doi.org/10.1039/c9en01089k.

Minussi, R.C., Pastore, G.M., Durán, N., 2002. Potential applications of laccase in the food industry. Trends Food Sci. Technol. 13 (6–7), 205–216. https://doi.org/10.1016/S0924-2244(02)00155-3.

Mogharabi, M., Faramarzi, M.A., 2014. Laccase and laccase-mediated systems in the synthesis of organic compounds. Adv. Synth. Catal. 356 (5), 897–927. https://doi.org/10.1002/adsc.201300960.

Natalio, F., André, R., Hartog, A.F., Stoll, B., Jochum, K.P., Wever, R., Tremel, W., 2012. Vanadium pentoxide nanoparticles mimic vanadium haloperoxidases and thwart biofilm formation. Nat. Nanotechnol. 7 (8), 530–535. https://doi.org/10.1038/nnano.2012.91.

Nath, I., Chakraborty, J., Verpoort, F., 2016. Metal organic frameworks mimicking natural enzymes: a structural and functional analogy. Chem. Soc. Rev. 45 (15), 4127–4170. https://doi.org/10.1039/C6CS00047A.

Peña, M.A., Fierro, J., 2001. Chemical structures and performance of perovskite oxides. Chem. Rev. 101 (7), 1981–2018. https://doi.org/10.1021/cr980129f.

Song, F., Schenk, K., Hu, X., 2016. A nanoporous oxygen evolution catalyst synthesized by selective electrochemical etching of perovskite hydroxide CoSn (OH) 6 nanocubes. Energy Environ. Sci. 9 (2), 473–477. https://doi.org/10.1039/C5EE03453A.

Song, D., Tian, T., Yang, X., Wang, L., Sun, Y., Li, Y., Huang, H., 2023. Smartphone-assisted sensor array constructed by copper-based laccase-like nanozymes for specific identification and discrimination of organophosphorus pesticides. Food Chem. 424, 136477 https://doi.org/10.1016/j.foodchem.2023.136477.

Strong, P., Claus, H., 2011. Laccase: a review of its past and its future in bioremediation. Crit. Rev. Environ. Sci. Technol. 41 (4), 373–434. https://doi.org/10.1080/10643380902945706.

Tang, J., Daiyan, R., Ghasemian, M.B., Idrus-Saidi, S.A., Zavabeti, A., Daeneke, T., Yang, J., Koshy, P., Cheong, S., Tilley, R.D., 2019. Advantages of eutectic alloys for creating catalysts in the realm of nanotechnology-enabled metallurgy. Nat. Commun. 10 (1), 4645. https://doi.org/10.1038/s41467-019-12615-6.

Tran, T.D., Nguyen, P.T., Le, T.N., Kim, M.I., 2021. DNA-copper hybrid nanoflowers as efficient laccase mimics for colorimetric detection of phenolic compounds in paper microfluidic devices. Biosens. Bioelectron. 182, 113187 https://doi.org/10.1016/j.bios.2021.113187.

Wang, Y., He, C., Li, W., Zhang, J., Fu, Y., 2017. Catalytic performance of oligonucleotide-templated Pt nanozyme evaluated by laccase substrates. Catal. Lett. 147, 2144–2152. https://doi.org/10.1007/s10562-017-2106-5.

Wang, J., Huang, R., Qi, W., Su, R., Binks, B.P., He, Z., 2019a. Construction of a bioinspired laccase-mimicking nanozyme for the degradation and detection of phenolic pollutants. Appl. Catal., B 254, 452–462. https://doi.org/10.1016/j.apcatb.2019.05.012.

Wang, X., Gao, X.J., Qin, L., Wang, C., Song, L., Zhou, Y.-N., Zhu, G., Cao, W., Lin, S., Zhou, L., 2019b. Eg occupancy as an effective descriptor for the catalytic activity of perovskite oxide-based peroxidase mimics. Nat. Commun. 10 (1), 704. https://doi.org/10.1038/s41467-019-08657-5.

Wang, Z., Wu, J., Zheng, J.-J., Shen, X., Yan, L., Wei, H., Gao, X., Zhao, Y., 2021. Accelerated discovery of superoxide-dismutase nanozymes via high-throughput computational screening. Nat. Commun. 12 (1), 6866. https://doi.org/10.1038/s41467-021-27194-8.

Wang, J., Huang, R., Qi, W., Su, R., He, Z., 2022a. Construction of biomimetic nanozyme with high laccase-and catecholase-like activity for oxidation and detection of phenolic compounds. J. Hazard Mater. 429, 128404 https://doi.org/10.1016/j.jhazmat.2022.128404.

Wang, Q., Wang, X., Wei, H., 2022b. Spinel-oxide-based laccase mimics for the identification and differentiation of phenolic pollutants. Anal. Chem. 94 (28), 10198–10205. https://doi.org/10.1021/acs.analchem.2c01695.

Wang, J., Han, J., Wang, J., Lv, X., Fan, D., Dong, S., 2024a. A cost-effective, "mix & act" G-quadruplex/Cu (II) metal-nanozyme-based ratiometric fluorescent platform for highly sensitive and selective cysteine/bleomycin detection and multilevel contrary logic computing. Biosens. Bioelectron. 244 https://doi.org/10.1016/j.bios.2023.115801.

Wang, K., Meng, X., Yan, X., Fan, K., 2024b. Nanozyme-based point-of-care testing: revolutionizing environmental pollutant detection with high efficiency and low cost. Nano Today 54. https://doi.org/10.1016/j.nantod.2023.102145.

Witayakran, S., Ragauskas, A.J., 2009. Synthetic applications of laccase in green chemistry. Adv. Synth. Catal. 351 (9), 1187–1209. https://doi.org/10.1002/adsc.200800775.

Wu, H., Lu, Q., Li, Y., Zhao, M., Wang, J., Li, Y., Zhang, J., Zheng, X., Han, X., Zhao, N., 2022. Structural framework-guided universal design of high-entropy compounds for efficient energy catalysis. J. Am. Chem. Soc. 145 (3), 1924–1935. https://doi.org/10.1021/jacs.2c12295.

Wulff, G.n., Liu, J., 2012. Design of biomimetic catalysts by molecular imprinting in synthetic polymers: the role of transition state stabilization. Acc. Chem. Res. 45 (2), 239–247. https://doi.org/10.1021/ar200146m.

Yang, L., Guo, X.-Y., Zheng, Q.-H., Zhang, Y., Yao, L., Xu, Q.-X., Chen, J.-C., He, S.-B., Chen, W., 2023. Construction of platinum nanozyme by using carboxymethylcellulose with improved laccase-like activity for phenolic compounds detection. Sens. Actuators B Chem. 393, 134165 https://doi.org/10.1016/j.snb.2023.134165.

Yu, J., Liu, Q., Qi, L., Fang, Q., Shang, X., Zhang, X., Du, Y., 2024. Fluorophore and nanozyme-functionalized DNA walking: a dual-mode DNA logic biocomputing platform for microRNA sensing in clinical samples. Biosens. Bioelectron. 252 https://doi.org/10.1016/j.bios.2024.116137, 116137-116137.

Zhang, R., Yan, X., Fan, K., 2021. Nanozymes inspired by natural enzymes. Acc. Mater. Res. 2 (7), 534–547. https://doi.org/10.1021/accountsmr.1c00074.

Zhang, M., Wang, Y., Li, N., Zhu, D., Li, F., 2023. Specific detection of fungicide thiophanate-methyl: a smartphone colorimetric sensor based on target-regulated oxidase-like activity of copper-doped carbon nanozyme. Biosens. Bioelectron. 237 https://doi.org/10.1016/j.bios.2023.115554.